Self-Assembling Structure in Solution of a Semirigid Polyelectrolyte

Wei Yang, Hidemitsu Furukawa, Yukari Shigekura, Kazuhiro Shikinaka, Yoshihito Osada, and Jian Ping Gong*

Division of Biological Sciences, Graduate School of Science, Hokkaido University, Sapporo 060-0810, Japan

Received June 5, 2007; Revised Manuscript Received December 25, 2007

ABSTRACT: We investigated the self-assembling structure in aqueous solution of polyelectrolyte poly(2,2′-disulfonyl-4,4′-benzidine terephthalamide) (PBDT), which has a rigid chemical structure of polyaramide in the main chain. It is found that PBDT exhibits a stretched semirigid conformation in solution, regardless of PBDT concentration, C_P, or salt addition. PBDT in water exhibits both a very low overlap concentration, C^*, and a lower critical concentration of nematic liquid crystal, C_{LC}^*. In the intermediate region of $C^* < C_P < C_{LC}^*$, PBDT forms cluster-like isotropic self-assembly. Moreover, in the intermediate region of $C^* < C_P < C_{LC}^*$, the addition of NaCl induces the alternation of structure from a cluster-like isotropic self-assembly to a fiber-like anisotropic one. Further addition of NaCl induces a network-like huge self-assembling structure, as the stoichiometric molar ratio of [NaCl] to [$NaSO_3^-$] increases beyond 1. The semirigid polyelectrolyte probably has hidden potential for structural polymorphism in aqueous solutions in the presence of salt.

Introduction

Water-soluble semirigid macromolecules in living organisms, such as deoxyribonucleic acid (DNA), actin filaments, and polysaccharides with double or triple helix structures, take quite important roles. They have great abilities to form well-ordered structures by spontaneous self-assembly, which is fundamental to invoke their biological functions. Hence, it is also interesting to find and control the hidden mechanisms that determine the well-ordered structures of semirigid macromolecules in living organisms.[1−6] From this point of view, the nature of synthetic semirigid polyelectrolyte should be studied further. However, it is essentially difficult to study it due to the complicated competition of the two different interactions, that is, short-range (excluded volume) interaction and long-range (electrostatic) one. The competition between them often causes complicated structures, which are related to not only the local structural formation along the polyelectrolyte chain[7,8] but also the self-assembly among the polyelectrolyte chains. On the other hand, some well-ordered structures were observed for a rigid polyelectrolyte.[9−19] We think that this unique behavior of a rigid polyelectrolyte is the key to elucidate the hidden mechanism of spontaneous self-assembly to form well-ordered structures in living organisms.

From this point of view, we have recently focused on the characterization of a kind of typical water-soluble semirigid polyelectrolyte with a main chain of poly(2,2′-disulfonyl-4,4′-benzidine terephthalamide) (PBDT).[20,21] In the previous studies, we found many specific features of PBDT, which probably originate from both the semirigidity and the highly charged polyelectrolyte properties of PBDT.

(1) In dilute aqueous solution of PBDT below a crossover concentration C^* of ∼0.3 wt %, the reduced viscosity in the salt-free condition shows a simple increase when the concentration is approximately 0. Thus, in the case of PBDT, the intrinsic viscosity can be determined with a value of 9.5 dL/g. This behavior is different from that of the diluted aqueous solution of the flexible polyelectrolyte. The reduced viscosity of the flexible polyelectrolyte shows an anomalous increase as the polymer concentration decreases. It is usually difficult to determine the reduced viscosity of flexible polyelectrolyte without the addition of salt.

(2) In a semidilute aqueous solution of PBDT above C^*, a steep increase in the reduced viscosity is observed as the polymer concentration increases. This is different from either a flexible polyelectrolyte or a completely rigid polyelectrolyte. In a semidilute aqueous solution of flexible polyelectrolyte, the reduced viscosity decreases as the polymer concentration increases, due to the screening effect. In a semidilute aqueous solution of completely rigid polyelectrolyte, the increase in the reduced viscosity is suppressed, because the conformation is not altered significantly.

(3) An aqueous solution of PBDT shows a nematic liquid crystalline state above a lower critical concentration, C_{LC}^*, of 2.8 wt %,[22] quite lower than those of common lyotropic liquid crystalline (LC) macromolecules. For instance, cellulose derivatives[23] generally show the LC state with a C_{LC}^* of about 20 wt % and the synthetic polyaramide, Kevlar, which has an elementary molecular structure similar to that of PBDT, shows the LC state with a C_{LC}^* of about 10 wt % in concentrated sulfuric acid.[24] The quite low C_{LC}^* of PBDT should be attributed to its intrinsic structural rigidity and its polyelectrolyte nature.

(4) A drastic increase in the reduced viscosity of PBDT for both below and above C_{LC}^* is observed when the salt (NaCl) concentration is above 10^{-2} M. This is also completely different from the flexible polyelectrolyte system, in which the reduced viscosity simply decreases with an increase in the salt concentration due to the screening effect of electrostatic repulsion.

(5) We recently found that anisotropic gels can be successfully synthesized from the cationic monomer *N*-[3-(*N*,*N*-dimethylamino)propyl]acrylamide methyl chloride quaternary (DMAPAA-Q) in the presence of a small amount of anionic PBDT.[25] It is interesting to find that an isotropic DMAPAA-Q monomer solution shows birefringence due to its anisotropic structure after gelation in the presence of PBDT. Furthermore, the prepared gels maintain birefringence after swelling in a large amount of water, while the PBDT concentration in the gels is quite below C_{LC}^*. Various analyses revealed that the existence of a large-size structure in a monomer solution with semirigid polyelec-

* Corresponding author. E-mail: gong@sci.hokudai.ac.jp.

10.1021/ma071251w CCC: $40.75
Published on Web 02/12/2008

trolyte is essentially important to induce birefringence during gelation. The possible mechanism of the anisotropic structure formation during gelation seeded by a semirigid polyelectrolyte is proposed based on the results of these observations.[26]

These interesting phenomena (1−5) are still not well understood, especially the large-size structure in the PBDT solution observed before gelation. In the present study, we focus on the structures of the association that form spontaneously when the polyelectrolyte (PBDT) is in a salt-free condition and in a sodium salt aqueous solution. The major method of investigation is the use of scanning microscopic light scattering (SMILS),[27−30] which could provide structural information in the length scale of several nanometers to several μm. Transmission electron microscopy (TEM) has been employed for the direct visualization of the structure of PBDT molecular association. Polarizing optical microscopy (POM) has been used to characterize the orientation at a molecular scale to confirm liquid crystalline structures.

Experimental Section

1. Sample Preparation. PBDT was prepared by an interfacial poly condensation reaction, as described elsewhere.[21] The aqueous solutions of PBDT were prepared by the "dilution" method. A mother solution was prepared at 5 wt % and subsequently diluted with pure solvent (water) in order to achieve a range of lower concentrations. On the other hand, PBDT + NaCl solutions in water were prepared according to a "direct dissolution" method consisting of preparing PBDT aqueous solutions with various PBDT concentrations by directly dissolving proper amounts of NaCl powder to achieve predetermined concentrations. Water was deionized and purified with 0.22 μm and 5 μm membrane filters before use.

2. GPC Analysis. Gel permeation chromatography (GPC) was performed with a HITACHI L-7110 pump and a HITACHI 7490 RI detector using a SHODEX OHpak SB-805HQ column and 0.5 M CH_3COOH + 0.2 M $NaNO_3$ as the elution solvent. Poly(sodium *p*-styrenesulfonate) (PNaSS) was used as a GPC standard. The weight-average molecular weight, M_w, number-average molecular weight, M_n, and polydispersity (M_w/M_n) of PBDT were 102 000, 88 000, and 1.2, respectively. From these results, the polymerization degree, N, was estimated as 170.

3. Structure Characterization. Dynamic Light Scattering (DLS). Scanning microscopic light scattering (SMILS) was carried out to scan and measure many different positions in the samples, in order to rigorously determine a time- and space-averaged, i.e., ensemble-averaged, (auto-) correlation function of the concentration fluctuating in the sample. All the samples of PBDT and PBDT + NaCl aqueous solutions were filtered through 0.1 μm filters to avoid interference from dust particles. An He−Ne laser with a 633 nm wavelength and a semiconductor laser with 532 nm wavelength were used in different solutions as the incident beam. Measurements were made at four different angles, which were 40, 60, 90, and 125°, and the typical measurement time was 90 s. The samples were maintained at a constant temperature of 30 °C throughout the experiments. Scanning measurement was performed at 31 points for each sample to determine the dynamic component of the ensemble-averaged dynamic structure factor $\Delta g_{en}^{(1)}(\tau)$.[27] The determined correlation function was transformed to the distribution function of relaxation time, $P(\tau_R)$, by using numerical inversed Laplace transform calculation.

The same SMILS system was used for depolarized DLS, where the polarized incident beam was set vertically and the scattered light was observed horizontally using a polarizer; henceforth, we call this depolarized setting HV and the normal setting VV.

On the basis of scattering theory, the characteristic relaxation time at the peak of the distribution function, τ_R, is used to determine the average translational diffusion coefficient D from $D = 1/(q^2\tau_R)$, where q is the scattering vector. The characteristic size of the diffusing objects, ξ, is related to D via the Einstein−Stokes equation, $D = k_BT/6\pi\eta\xi$, where k_B is the Boltzmann constant and η is the viscosity of the solvent at the absolute temperature T.

Observation and Measurement with Polarized Optical Microscopy (POM). Samples were sandwiched between two glass plates and the upper surfaces were observed by a crossed polarizing microscope (Olympus, BH-2) at room temperature. Birefringence, Δn, was measured using a crossed polarizing microscope with a Berek compensator for the retardation[31] and the average of 5 measurements was recorded for each sample. In the measurement, many microscopic domains randomly oriented in the bulk were observed. We chose one of the largest domains and selected its orientation direction by turning the sample under the crossed polarizing microscope.

Transmission Electron Microscopy (TEM) Observation. Transmission electron microscope (TEM) characterization was conducted using a JEOL (JEM-1200EX) system operating at a 120 kV acceleration voltage. The samples, which were the same solutions as those used for the DLS experiments, were fixed on a carbon-coated copper grid (NISSHIN EM Co., Tokyo). The samples generally had to be diluted with pure solvent to achieve concentrations compatible with the TEM sample preparation technique. Most of the water was removed by touching the grid edge to a filter paper wedge, and the sample was allowed to dry in the open under room conditions. Since these structures are concentration dependent, all the experimental procedures were performed rapidly to maintain the C_P in order to ensure correlation with the DLS measurements.

In order to increase the contrast of the sample in TEM, additional staining was employed. After the excess solvent had been carefully removed by blotting with the edge of a filter paper and subsequent evaporation at room temperature, 2 wt % uranyl acetate was added to the sample without change in the structural properties. Afterward, the samples in which the excess stain was removed by blotting with a filter paper wedge were allowed to air-dry at room temperature.

Results and Discussion

1. Effect of PBDT Concentration. First, we should note the counterion behavior in the PBDT aqueous solution. According to Manning−Oosawa's condensation theory,[32,33] when the polyelectrolyte charge density is higher than a critical value in which the electrostatic repulsive energy between the next neighboring charges along the polyelectrolyte is higher than the thermal fluctuation energy, some of the counterions will be strongly localized and will condense near the polyelectrolyte. The critical condition for counterion condensation is characterized by a variable q

$$q = \lambda_B/l_e \tag{1}$$

Here, l_e, is the characteristic length related to the charge density along the polyelectrolyte, and λ_B is the Bjerrum length, the critical length between charged groups along the polyelectrolyte chain for Manning−Oosawa counterion condensation

$$\lambda_B = e^2/4\pi\epsilon k_BT \tag{2}$$

Here e is the elementary charge; ϵ, the solvent dielectric constant; k_B, Boltzmann's constant; and T, the absolute temperature. q is an inherent characteristic function and independent of the polyelectrolyte concentration. The counterion condensation occurs when $q > 1$. For PBDT, l_e is approximately equal to $a/2 = 8$ Å because the PBDT repeat-unit size a is 1.6 nm.[25] For an aqueous solution at the room temperature, the Bjerrum length could be calculated as $\lambda_B = 7$ Å. Thus, with eq 1, the q value is slightly lower than 1, which means that the counterions could hardly condense near the PBDT polyelectrolyte in the present case.

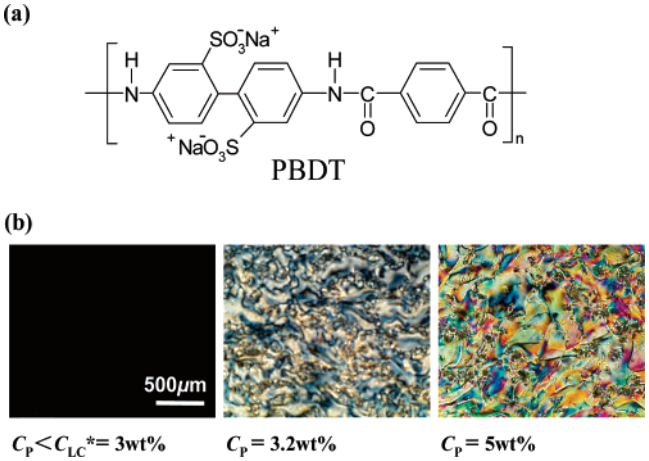

Figure 1. (a) Chemical structure of the PBDT. (b) POM images of PBDT aqueous solutions at various concentrations of PBDT, C_P, around the lower critical concentration of lyotropic liquid crystal, $C_{LC}^* = 3$ wt %.

Figure 1 shows crossed polarizing microscope images of PBDT aqueous solutions at various PBDT concentrations, C_P. A strong birefringence and the schlieren texture of the nematic LC phase could be observed when $C_P \geq 3$ wt %. This means that there is a critical PBDT concentration C_{LC}^* for showing the LC nature; this concentration is in agreement with our previous results.[22] For rigid-rod LC molecules, the critical volume fraction for showing the LC nature, ϕ_{LC}^*, is estimated by Flory's lattice theory as

$$\phi_{LC}^* = \frac{8}{X}\left(1 - \frac{2}{X}\right) \cong \frac{8}{X} \tag{3}$$

Here, X is the axial ratio as defined by the equation

$$X = \frac{L}{D} \tag{4}$$

where L is the length of the molecules and D is the width of the molecules. Here, the volume fraction of polymer ϕ is simply related to the concentration of polymer C by the equation

$$C = \phi \times \frac{\rho_P}{\rho_S} \tag{5}$$

where ρ_P and ρ_S ($\rho_P = 1.3$ g/cm^3 and $\rho_S = 1.0$ g/cm^3) are the densities of the PBDT polymer and the aqueous solutions, respectively. By using eqs 3 and 5, we obtain $X \cong 347$ when $C_{LC}^* = 3$ wt %. If we let $L = aN$, $X = L/D = (a/D)N$ will be obtained. Since we can assume $a/D \sim 1$ and $N = 170$ is estimated by GPC, it strongly suggests that PBDT becomes almost fully stretched when its LC nature emerges. Thus, we find that in the present case, C_{LC}^* is inversely proportional to the polymerization degree, N, by eq 6.

$$\phi_{LC}^* \cong 8/X^{-1} \propto X^{-1} \propto N^{-1} \tag{6}$$

In order to obtain detailed structural information in several nanometers to several μm, DLS analysis was performed. Figure 2a shows the dynamic component of the ensemble-averaged dynamic structure factor $\Delta g_{en}^{(1)}(\tau)$ of the 3.2 wt % PBDT solutions at four different scattering angles. Figure 2b presents the q^2-scaled plot of $\Delta g_{en}^{(1)}(q^2\tau)$. It is shown that the q^2-scaled $\Delta g_{en}^{(1)}(q^2\tau)$ converges well onto a curve. This means that all the

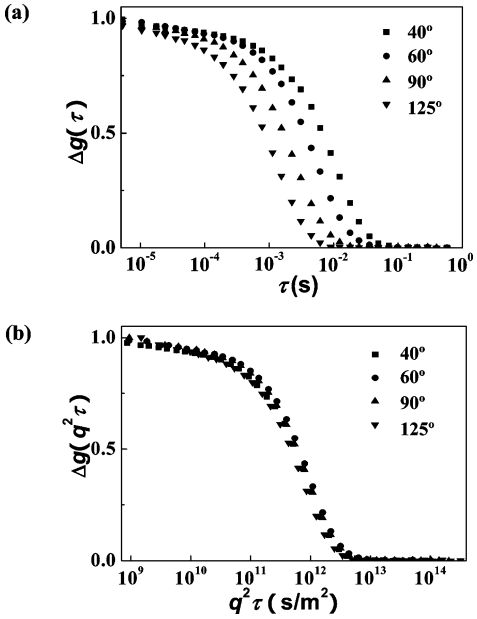

Figure 2. (a) Correlation function, $\Delta g(\tau)$, of 3.2 wt % PBDT solutions at four different scattering angles, observed by DLS ($\lambda = 633$ nm, $\theta = 40$, 60, 90 and 125°). (b) q^2-scaled plot of $\Delta g(q^2\tau)$, showing the diffusive nature of the correlation function of Figure 2a.

relaxation processes of $\Delta g_{en}^{(1)}(\tau)$ can be attributed to the translational diffusion process.

The distribution function of relaxation time, $P(\tau_R)$, is shown in Figure 3a. All the samples show a relaxation peak and the peak position exhibits a right-shift as the concentration increases, which means that a higher concentration corresponds to a slower relaxation time τ_R. Otherwise, under higher concentrations, other small contributions are observed around $10^{-3}-10^{-4}$ s. This is attributable to the coexistence of different structures of free and associated PBDT. For all the samples, we confirmed that the observed relaxation modes have q^2 dependence, indicating that the relaxation modes originate from the translational diffusion process. The translational diffusion coefficient D and the characteristic sizes ξ are estimated, as shown in Figure 3b. It is obvious that the observed characteristic size depends on the PBDT concentration and changes in three different concentration regions: (i) in the region of PBDT concentration $C_P \leq 0.3$ wt %, ξ can be determined with minimum values of ~43 nm; (ii) in the region 0.3 wt % $< C_P <$ 3 wt %, ξ increases with the concentration; (iii) in the region $C_P > 3$ wt %, just above C_{LC}^*, ξ becomes almost constant again at around a value of 1.4 μm. The change in ξ with an increase in C_P is in good agreement with the reduced viscosity change observed in our previous work,[22] as shown in Figure 3c. In addition, in Figure 3c, the viscosity behavior of a flexible polyelectrolyte, poly(2-acrylamido-2-methylpropanesulfonic acid) (PAMPS),[22] is shown for comparison. The flexible polyelectrolyte shows a steep, monotonic decrease in reduced viscosity with an increase in C_P, as mentioned in the Introduction. Meanwhile, when the PBDT concentration is above ~0.3 wt %, the increases in both the reduced viscosity and the characteristic size ξ with an increase in C_P are observed. This strongly suggests the formation of a different large-size structure due to the change in the PBDT interchain interactions above this C_P. Here, it should be noted that in order to estimate the characteristic length ξ from D by the Stokes−Einstein relation, we should use not the solvent viscosity but the solution viscosity. However, if we use the solution viscosity in the present study, the value of the characteristic length becomes unreasonable; this is difficult to

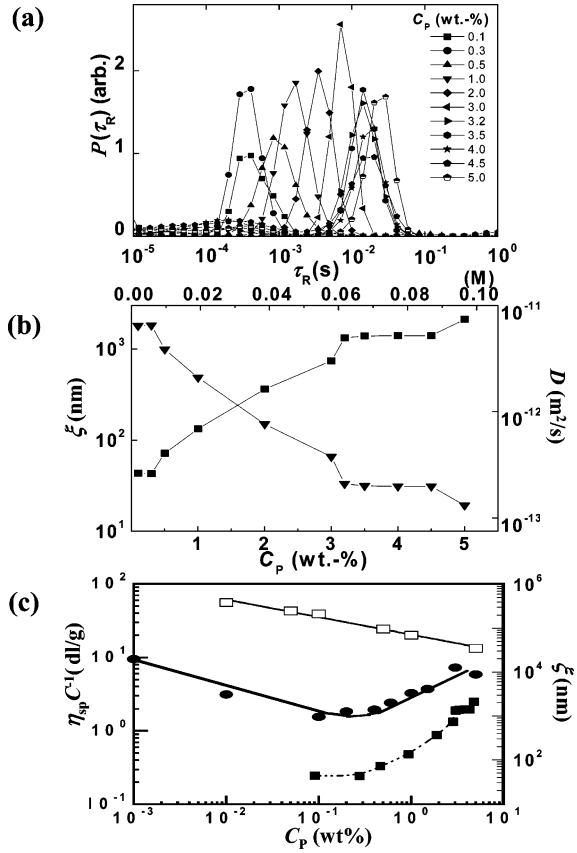

Figure 3. (a) Distribution function of relaxation time, $P(\tau_R)$, of PBDT aqueous solutions at different concentrations observed by DLS (λ = 633 nm, θ = 90°). (b) PBDT concentration, C_P, dependence of the correlation length ξ (■) and the translational diffusion coefficient D (▼). (c) PBDT concentration, C_P, dependence of the reduced viscosity[22] $\eta_{sp}C^{-1}$ for PBDT (●) and PAMPS (▼) and the correlation length ξ (■) for PBDT. The ξ is the same one plotted in (b).

discuss with any attribution to the actual structure. Thus, in order to have only a simple comparison with the other results, the characteristic length ξ was simply estimated by using the solvent viscosity.

Here, we discuss what the observed characteristic size ξ stands for. If we consider L to be the hydrodynamic radius, approximately, the characteristic size ξ observed in the region $C_P \leq 0.3$ wt % will roughly give the diameter as $L = 2\xi = 86$ nm; this L is much smaller than L_{ROD}, which is equal to $a \cdot N = 272$ nm, analyzed completely in terms of an individual rigid rod. Moreover, on the basis of our previous studies about the reduced viscosity in a dilute aqueous solution of PBDT showing a simple increase below the crossover concentration C^* of ~0.3 wt %, which is different from the diluted aqueous solution of a flexible polyelectrolyte, we can assume that the PBDT molecules are semirigid and exist in the state of a single molecule without association in the dilute region ($C_P < 0.3$ wt %).

The characteristic size ξ increases with the PBDT concentration in the region 0.3 wt % < C_P < 3 wt %, which distinctly indicates the formation of molecular association. On the other hand, contrary to Manning−Oosawa's counterion condensation theory, the counter-ions could hardly condense on the PBDT poly ions. Thus, a strong electrostatic interaction exists between the PBDT chains that prevent association. We consider that the molecular association before C_{LC}* originates from the hydrophobic nature of the PBDT main chain backbone or from the hydrogen bonds between PBDT main chains, which compete with the osmotic repulsion. Otherwise, it is noted that macromolecular packing does not occur in conventional flexible polyelectrolytes such as PAMPS, while in the case of semirigid PBDT with aromatic rings, macromolecular association has been identified. Therefore, we think that the effect of the aromatic rings on the formation of molecular association could also not be neglected.

To confirm the results of DLS analysis, we tried to observe the structure of PBDT molecular association directly by TEM. Figure 4 shows the TEM images of PBDT aqueous solutions at four different concentrations. Although the actual structure of PBDT association in water should be somewhat different from that observed in the TEM images, since the concentration gradually increases with time under the experimental procedure, we can obtain valuable information about some specific large-structures of PBDT in solution via the same procedure. Then, it is obvious that the PBDT molecules are properly monodispersed in a highly diluted condition of $C_P = 0.1$ wt % (Figure 4a), and the semirigid conformation of PBDT is observed. For $C_P = 0.5$ wt % (Figure 4b), some dispersed cluster-like association is observed. This confirms that the association of PBDT began to form even at a concentration far below C_{LC}*. When C_P is close to C_{LC}* (Figure 4c), snow-like structures are observed. When C_P is increased to 5 wt %, above the C_{LC}*, bundle-like aggregates with uniform orientation are formed (Figure 4d). The sizes of the aggregate structures at different concentrations are reasonably consistent with the DLS results. On the other hand, by comparing the TEM photographs at a lower magnification, we find that both the anisotropy and continuity of the molecular association are improved by the increase in C_P.

Furthermore, it is noted that objects sometimes appear white or black in the TEM images. We consider that this is substantially influenced by the nature of the superstructures, which is responsible for the location of an additional negative stain. The principle of negative staining relates to the imaging of a thinly spread particulate material by surrounding it with a heavy-metal salt in solution and allowing the solution to dry, thereby embedding the material in an amorphous electron-dense layer. We may, thus, identify the formed structures observed in Figure 4, parts b−d, to be composed of several individual PBDT molecules, where the aggregates are not strongly bonded together and a negative stain can surround each individual bonded loosely so that it appears white. In contrast to this, in a highly diluted condition of $C_P = 0.1$ wt % (Figure 4a), only monodispersed threadlike structures (black) were observed, once again suggesting that the PBDT molecules are semirigid and exist in a single molecule state without association in the dilute region ($C_P < 0.3$ wt %).

In order to elucidate how the orientation changes within different PBDT molecular associations above C_{LC}*, we measured the birefringence of different solutions with concentrations above C_{LC}*, $\Delta n = n_{\parallel} - n_{\perp}$. As shown in Figure 5(●), Δn increases continuously with C_P, although the DLS results show that a characteristic size is almost constant in this concentration region. We further found that the order parameter ($\Delta n/100C_P$), a characteristic order parameter for the orientation of the solution, increases with the concentration (Figure 5(▼). This result indicates that when the PBDT concentration is higher than C_{LC}*, although the characteristic size of molecular association remains constant, the orientation of the molecular association within the LC domain steeply increases with C_P.

On the basis of the above experiments and discussions, we can summarize that a PBDT aqueous solution changes its structure in three concentration regions, which are characterized

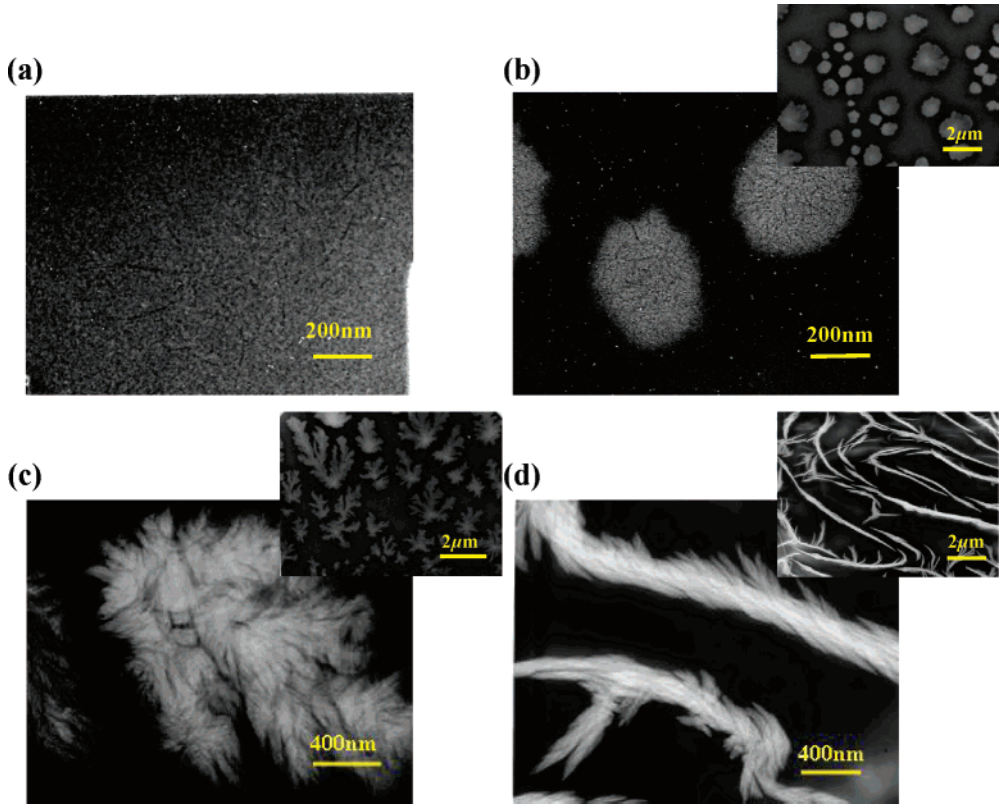

Figure 4. TEM images of PBDT association of various PBDT concentrations, C_P, around the crossover concentration of PBDT, C^*, and the lower critical concentration of lyotropic liquid crystal, C_{LC}^*. (a) $C_P = 0.1$ wt % ($C_P < C^*$), (b) $C_P = 0.5$ wt % ($C^* < C_P < C_{LC}^*$), (c) $C_P = 3$ wt % ($C_P \approx C_{LC}^*$), and (d) $C_P = 5$ wt % ($C_P > C_{LC}^*$). Although the magnified image of part b was once shown in the previous study,[26] it is shown again here to make a clear comparison to the other conditions.

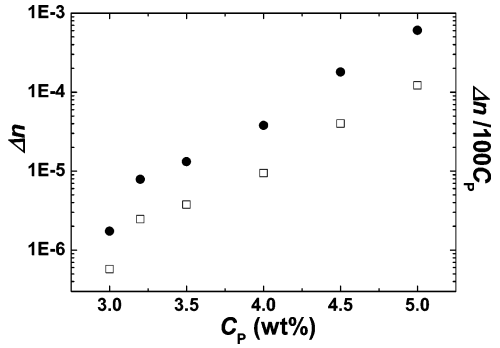

Figure 5. PBDT concentration, C_P, dependence of birefringence, $\Delta n = n_{\parallel} - n_{\perp}$ (●) and order parameter, $\Delta n/100C_P$ (▼) of the PBDT aqueous solutions in high C_P region above the lower critical concentration of lyotropic liquid crystal, C_{LC}^* ($C_P \geq C_{LC}^*$).

by the crossover concentration, C^*, and the liquid crystalline concentration, C_{LC}^*.

(i) When $C_P < C^*$, PBDT molecules exist in a single molecule state, without molecular association. The reduced viscosity decreases with an increase in C_P due to the semirigid nature of the PBDT.

(ii) When $C^* < C_P < C_{LC}^*$, PBDT molecules form associations and the size of these association increases with the PBDT concentration. The reduced viscosity increases with an increase in C_P due to molecular association.

(iii) When $C_P > C_{LC}^*$, the characteristic size of fluctuating molecular association remains constant in a certain concentration region again. The reduced viscosity shows a continuous increase with an increase in C_P.

2. Effect of Salt. The added salts always play an important role in determining the solution behavior of a polyelectrolyte. For a conventional flexible polyelectrolyte, with an increase in the salt concentration, the viscosity decreases because the electrostatic repulsion between the next neighboring polyions is screened and the polyelectrolyte chains shrink. As previously mentioned in the Introduction, some abnormal and unique phenomena for the PBDT solution have been observed in the presence of NaCl.[22] For PBDT, because the chain is rigid but may become slightly flexible by the addition of salt, it is expected that the viscosity will slightly decrease with an increase in the salt concentration. This is confirmed in the 0.1 wt % (corresponding to $C_P < C^*$) dilute solution of PBDT, where PBDT exists in a single molecule form. For higher concentrations of 1 and 5 wt % (corresponding to $C^* < C_P < C_{LC}^*$ and $C_P > C_{LC}^*$, respectively), the reduced viscosity shows a drastic increase with an increase in the salt concentration above a certain level, which suggests that the PBDT structure undergoes a dramatic change with the added salt.[22]

To clarify the structure in the presence of NaCl, we performed the DLS analysis of $C^* < C_P < C_{LC}^*$ and $C_P > C_{LC}^*$ solutions. The distribution functions of relaxation time, $P(\tau_R)$, of the 1 wt % ($C^* < C_P < C_{LC}^*$) PBDT solution at various NaCl concentrations are shown in Figure 6a. For all the NaCl concentrations, two relaxation peaks are observed. The peak position of the slow mode remains constant below a critical salt concentration of around 0.04 M, and above this salt concentration, the distribution of relaxation time widens and the peak exhibits a right-shift. From the relaxation times of the slow mode, the translational diffusion coefficient D and the characteristic sizes ξ at various NaCl concentrations are estimated, as shown in Figure 6b. The ξ of the 1 wt % PBDT

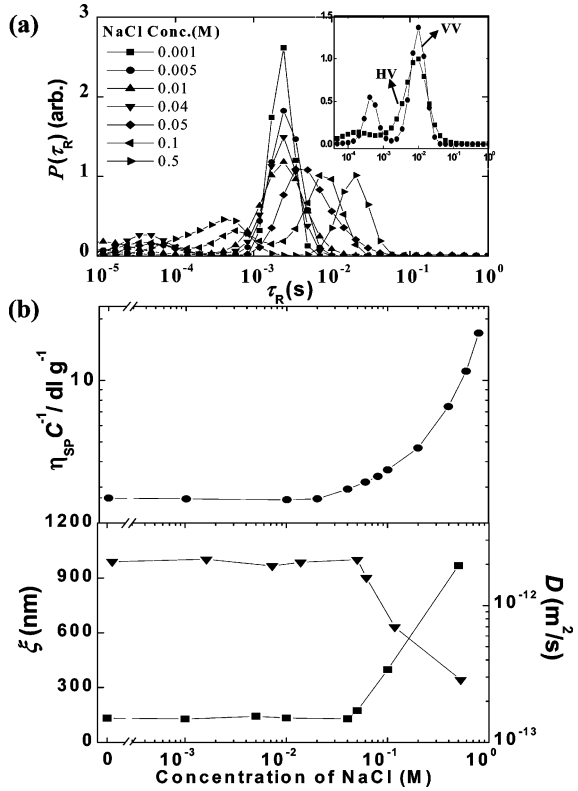

Figure 6. (a) Distribution function of relaxation time, $P(\tau_R)$, of 1 wt % PBDT in the presence of NaCl with various NaCl concentrations observed by DLS (λ = 633 nm, θ = 60°). The inset shows the depolarized DLS analysis in HV compared with the usual DLS in VV (1 wt % PBDT + 0.005 M NaCl). (b) NaCl concentration dependence of the reduced viscosity[22] $\eta_{sp}C^{-1}$ (●) and of the correlation length x (■) and the translational diffusion coefficient D (▼).

solution remains constant when the NaCl concentration is below 0.04 M, suggesting that the PBDT structure is not affected by the salt addition. However, this suggestion is not exact. As will be discussed below, the DLS-determined apparent size is maintained, while the detailed structure of PBDT association changes as the NaCl concentration increases below 0.04 M. Further, ξ steeply increases with the salt concentration above 0.04 M, indicating the formation of another large-size structure of PBDT. The DLS results agree well with our previous results, which showed that the reduced viscosity of 1 wt % PBDT solution greatly increases when NaCl is above 0.04 M, as shown in Figure 6b.[22] The fast relaxation mode is also observed in Figure 6a, which corresponds to the other small characteristic size ranging from 10 to 40 nm. This size is smaller than the molecular size of PBDT, so that it is probably related to the size of the inner structure in the molecular association. If the fast mode showed q^2 dependence, it could be attributed to a kind of cooperative diffusion in a network-like structure in an associated large-size structure, since the condition $q\xi > 1$ is satisfied.[26] However, the magnitude of the fast mode was too small to be discussed quantitatively here. As discussed according to Manning−Oosawa's condensation theory, we can consider that the counterions could hardly condense near the PBDT polyelectrolyte in the salt-free case. Since the q value is close to 1, however, it is expected that the added extra salt will tend to decrease the Debye screening length and weaken the repulsive force among PBDT molecules, which work to screen the electrostatic repulsion between the next neighboring polyion. Once the aggregation of PBDT molecules occurs, some of the counterions become trapped in the aggregates and then the aggregations are stabilized. Therefore, we changed the abscissa

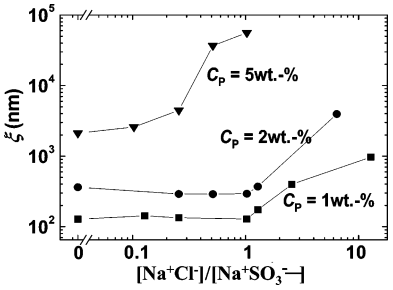

Figure 7. Molar ratio of the added salt concentration to the charge group of PBDT [Na^+Cl^-]/[$Na^+SO_3^-$] dependence of correlation length ξ for PBDT solution in the presence of NaCl. PBDT concentration, C_P, is varied as (■) 1, (●) 2 ($C^* < C_P < C_{LC}^*$), and (▼) 5 wt % ($C_P > C_{LC}^*$), where C^* is the crossover concentration of PBDT and C_{LC}^* is the lower critical concentration of lyotropic liquid crystal.

of Figure 6b from the added salt concentration to the molar ratio of the specific salt concentration to the charge group on the polymer, [Na^+Cl^-]/[$Na^+SO_3^-$], as shown in Figure 7. The steep increase in ξ is found to start exactly at a molar ratio of 1:1. A similar behavior is observed in the 2 wt % PBDT + NaCl system (Figure 7). These results indicate that this critical transition in the structure of PBDT association is due to the stoichiometric interaction between the added [Na^+Cl^-] and the charge group on the polymer [$Na^+SO_3^-$].

TEM images of the PBDT solution with various NaCl concentrations are shown in Figure 8. For 1 wt % PBDT aqueous solution with 0.001 M NaCl ([Na^+Cl^-]/[$Na^+SO_3^-$] < 1), the dispersed fiber-like aggregates are observed as shown in Figure 8a, and the aggregates seemed to be longer and thinner, as compared to those observed in a salt-free system, as shown in Figure 4a. In other words, we can assume that the shape of the aggregate tends to become more anisotropic, while it is almost isotropic in a salt-free system.

In order to elucidate this assumption, a depolarized DLS analysis in HV[26] was carried out to study whether the aggregate structure becomes anisotropic only with the addition of a small amount of NaCl. Here, the polarized incident beam was set vertically and the scatter light was observed horizontally using a polarizer. It should also be noted that here we used another PBDT, which was synthesized in the same way as that used in the present study at a different time, due to the diminution of the PBDT sample. Additionally, in this HV observation, we had to use a strong incident beam (λ = 532 nm at a scattering angle of 40°), which is different from the condition in the other DLS experiment in the present study. Therefore, we simply tried the qualitative observation of the PBDT structure. In the case of a salt-free PBDT aqueous solution (1 wt %), the relaxation peak was hardly observed in HV (not shown here). This means that the structure of PBDT association has an isotropic nature. For the PBDT 1 wt % + NaCl aqueous solution, at all NaCl concentrations, the slow mode was easily observed even in HV, the profile of which is quite similar to that of the slow mode observed by the usual (nondepolarized) DLS in VV; however, the fast relaxation mode was too weak to be observed in HV. These results are shown in the inset of Figure 6a, although the apparent relaxation time is different from the other observations due to the different DLS conditions. Furthermore, in order to prove that the depolarized light scattering does not arise from the intrinsic anisotropy or multiple scattering of PBDT in solution, we tried to analyze the slow mode in HV by assuming an ellipsoidal structure with $\Gamma_{VH} = 6D_r + Dq^2$, where D_r is the rotational diffusion coefficient and D is the translational diffusion coefficient.[14,17,19] Here, at all NaCl concentrations, Γ_{VH} is clearly q^2-dependent. However, the plot of Γ_{VH} vs q^2 has a

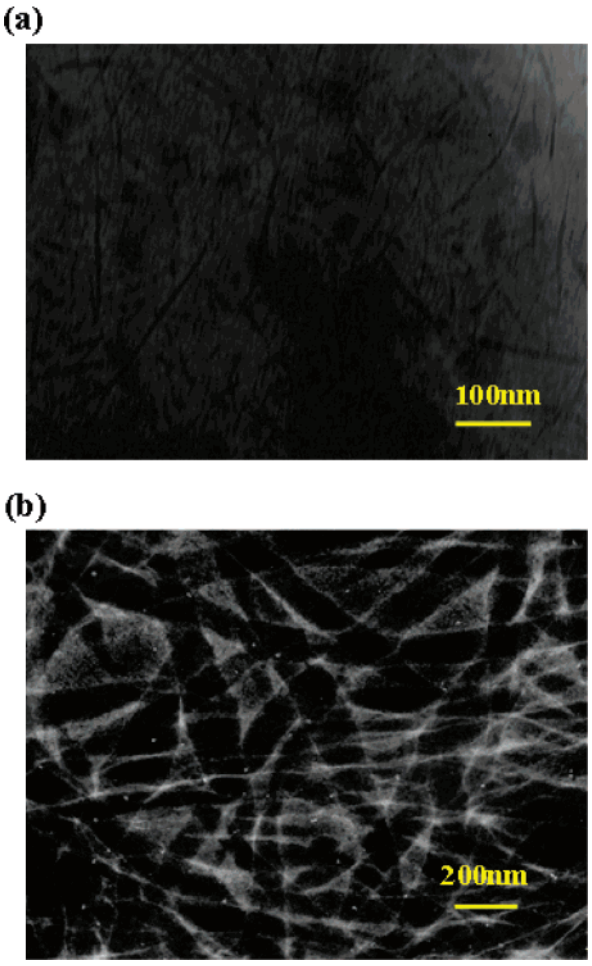

Figure 8. TEM images of the 1 wt % PBDT solutions ($C^* < C_P < C_{LC}^*$) in the presence of NaCl at 0.001 (a) and 0.5 M (b), where C^* is the crossover concentration of PBDT and C_{LC}^* is the lower critical concentration of lyotropic liquid crystal.

very small intercept (not shown here) that could not be distinguished from the errors; therefore, we cannot determine the rotational diffusion coefficient D_r. In spite of this, the q^2 dependence of Γ_{VH} strongly suggests that the HV relaxation, mainly due to the translational diffusion, originates from an anisotropic structure.

Although no size change was apparently observed by the usual (nondepolarized) DLS in VV as the salt concentration increased, as shown in Figure 6b, the structure transitioned from an isotropic cluster-like aggregate to an anisotropic fiber-like structure. This structural transition of aggregates by the addition of salt should be associated with the counterion screening effect on the PBDT interchain hydrogen bonding interactions within the domain association, which make it difficult for the polymer molecules to grow aggregates along the vertical direction of the polymer chains.

For 1 wt % PBDT aqueous solution with 0.5 M NaCl ($[Na^+Cl^-]/[Na^+SO_3^-] > 1$), we observe a network-like structure consisting of well-defined bundles (Figure 8b). It is noted that the objects appear black in the TEM images. This is completely different from the case of the salt-free condition, in which the objects appear white. Therefore, it cannot be inferred that in the bundles observed by TEM images, the polymer chains are strongly aligned and they are in close contact, so that they can subsequently accept the added negative stain. The negative stain only surrounds the bundles outside so that they appear white. From the TEM results, the characteristic size ξ, and the reduced viscosity data, we know that the addition of salt leads to a structural transition for the PBDT with $C^* < C_P < C_{LC}^*$, at $[Na^+Cl^-]/[Na^+SO_3^-] = 1$, where the dispersed anisotropic PBDT aggregates start to form a thick network-like structure.

The added salt effect on 5 wt % ($C_P > C_{LC}^*$) PBDT is shown in Figure 7 (▼). ξ increases with an increase in salt concentration, and there are no areas where the sizes are retained. This is not similar to the case of the $C^* < C_P < C_{LC}^*$. Furthermore, precipitates due to the salting out effect form when the charge ratio reaches 1:1. The liquid crystalline behavior also changes with the addition of salt, as revealed by the POM images in Figure 9. Although ξ increased continuously, as shown by the DLS results in Figure 7, the orientation of the structure vanished gradually as the salt concentration increased, as confirmed by the disappearance of birefringence. When the NaCl concentration is 0.05 M and higher, POM observation reveals discontinuous spotlike birefringence, which decreases in intensity and density with an increase in NaCl concentration (Figure 9c−f). This indicates the coexistence of two different phases: one being an oriented anisotropic structure, showing birefringence in POM, and the other being a nonoriented isotropic structure, not showing birefringence but a black background in POM. TEM images further confirm the structure observed by POM. As shown in Figure 4d, for salt-free 5 wt % PBDT aqueous solutions, bundle-like aggregates with uniform orientation are observed. When 0.2 M NaCl is added to the solution, the TEM images show two different morphologies: branched aggregates with certain ordered orientation (Figure 10, parts a and b) and random network-like structures (Figure 10c), which is in agreement with the POM images. Here, once again, the objects appear white in the TEM images, which is different from the case of the same added salt at 1 wt % PBDT + NaCl, suggesting that the bonds of PBDT loosen when $C_P > C_{LC}^*$.

From the above results, it is clear that the association structure of PBDT changes under the influence of the added salt. This salt effect might be responsible for the PBDT-induced anisotropic structure formation in polycation gels.[25] Cationic chloride monomer, DMAPAA-Q, acts as the added salt for PBDT to form the same structure as that in the present study when $C^* < C_P < C_{LC}^*$ and the charge ratio is >1. That is, nonoriented network-like structures, as shown in Figure 8b, are formed in the pregel solution. This is confirmed by a recent study, which demonstrates the formation of enormous network-like structures resulting from the screening effect of DMAPAA-Q as the added salt.[26] However, for enormous large network-like structures existing when $C_P > C_{LC}^*$, the orientation of the structure gradually vanished as the salt concentration increased. Therefore, from only the salt effect of DMAPAA-Q, it is still difficult to interpret how the little-oriented network-like structures in the pregel solution could spontaneously form well-oriented structures during the gelation process. We should continue the study of the PBDT system to clarify the mechanism of anisotropic gelation induced by PBDT.[26]

3. Phase Diagram of Self-Assembling Structure. We summarize the present work as a phase diagram of PBDT concentration C_P vs NaCl concentration C_s in Figure 11. For the salt-free PBDT aqueous solution, the sizes of the aggregate structures change in three concentration regions. In a dilute solution, PBDT is dispersed as a single rigid polyelectrolyte (Figure 11a). Even when the concentration is higher than the crossover concentration C^*, but still lower than the C_{LC}^*, the cluster-like isotropic molecular association is formed and the reduced viscosity of the solution also increases steeply as the PBDT concentration increases (Figure 11b). This result is quite

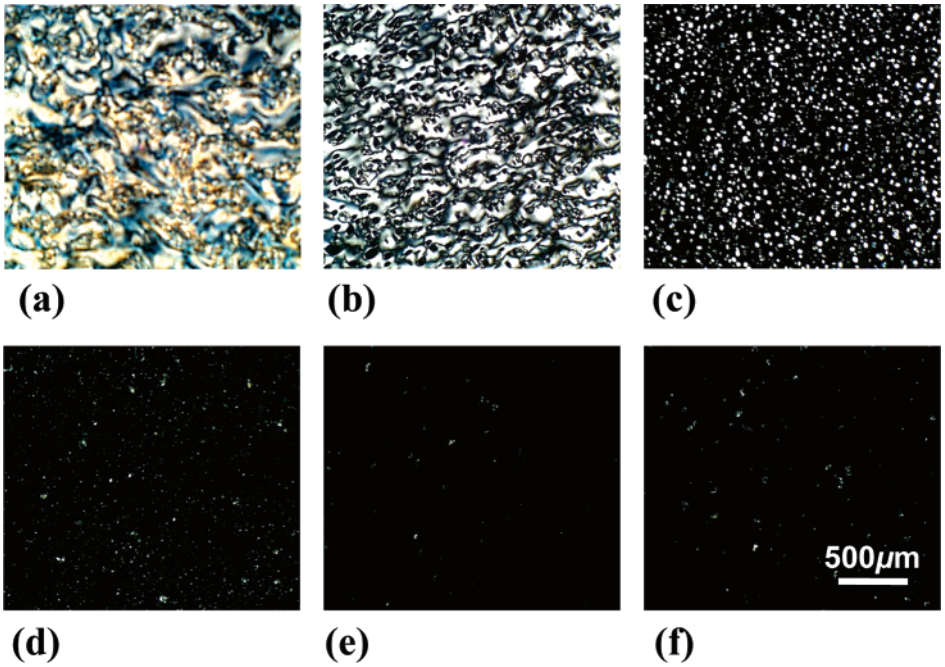

Figure 9. POM images of the 5 wt% PBDT solutions above the lower critical concentration of lyotropic liquid crystal, i.e., $C_P > C_{LC}^*$, in the presence of NaCl at various concentrations. NaCl concentration: (a) 0, (b) 0.02, (c) 0.05, (d) 0.1, (e) 0.2, and (f) 0.5 M.

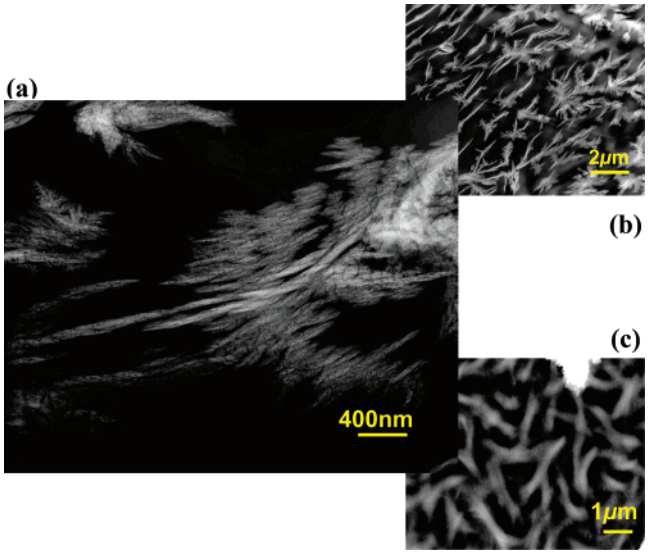

Figure 10. TEM images of the 5 wt % PBDT solutions above the lower critical concentration of lyotropic liquid crystal, i.e., $C_P > C_{LC}^*$, in pure water in 0.2 M NaCl aqueous solution. The left-hand side large image (a) is the corresponding enlarged one of part b. Right-hand side small images (b and c) are images observed at different positions in the same sample.

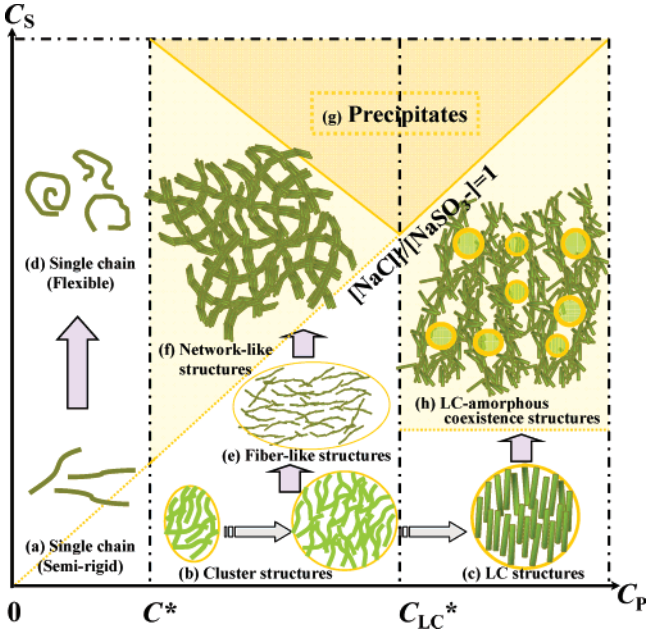

Figure 11. Phase diagram of PBDT concentration, C_P, vs NaCl concentration, C_s, where C^* is the crossover concentration of PBDT and C_{LC}^* is the lower critical concentration of lyotropic liquid crystal.

unexpected but interesting, because it has been proved that the Manning−Oosawa counterion condensation could hardly occur for a PBDT aqueous solution, which would result in strong electrostatic repulsion between PBDT polyions. It may be due to the hydrophobic interaction or hydrogen bonds between PBDT chains, which would be stronger than the electrostatic repulsive force when $C_P > C^*$. Further, as C_P increases beyond C_{LC}^*, the clusters start to overlap and form an anisotropic LC structure where the polymer chain is fully stretched (Figure 11c).

For the salt solution, in the dilute PBDT solution of $C_P < C^*$, the addition of salt alters the rigidity of PBDT so that it becomes slightly flexible; consequently, the reduced viscosity slightly decreases (Figure 11d). In the semidilute PBDT solution of $C^* < C_P < C_{LC}^*$, the cluster-like isotropic aggregates transition to a fiber-like anisotropic structure as C_s increases (Figure 11e), where the apparent size does not change and the reduced viscosity of the solution also does not change. However, as C_s increases further over a critical value of $[Na^+Cl^-]/[Na^+-SO_3^-] = 1$, PBDT forms a network-like structure from a fiber-like structure, so that the reduced viscosity steeply increases (Figure 11f). As C_s increases still further, PBDT begins to precipitate (Figure 11g). In a semi-concentrated PBDT solution of $C_P > C_{LC}^*$, the addition of salt destroys the LC phase, and the LC phase and the amorphous phase coexist (Figure 11h); the reduced viscosity also increases quickly. The LC phase vanishes as C_s increases. Subsequently, the precipitates also form

when the charge ratio exceeds the critical value of $[Na^+Cl^-]/[Na^+SO_3^-] = 1$ for $C_P > C_{LC}^*$ due to the salting-out effect (Figure 11g).

Conclusion

We found that PBDT behaves as a semirigid molecule in an aqueous solution and shows a variety of the self-assembling structures. It was confirmed that PBDT is free from the Manning−Oosawa condensation of counterion, so that the rigidity of the main chain hardly changes by the electrostatic screening due to the increase in polymer concentration as well as the addition of salt. However, both the increase in polymer concentration and the addition of salt induce various kinds of self-assembling structures. These features are quite different from those of a flexible polyelectrolyte. Moreover, PBDT exhibits two critical polymer concentrations of C^* and C_{LC}^*, so that there are three different regions divided by the two concentrations. We showed that the coexistence of two critical concentrations is essentially related to the stretched conformation of semirigid molecules. The addition of NaCl to the aqueous solution induces a different behavior in each of the three different regions. We also found that the stoichiometric molar ratio of [NaCl] to [PBDT] is crucial for the various self-assembling behaviors, which were classified into eight regions in the phase diagram of PBDT in solution in the presence of salt. This tells us that the semirigid polyelectrolyte has real potential for showing a rich variety of self-assembling structures. We hope the progress in the research of the various self-assemblies of a semirigid polyelectrolyte will clarify the crucial roles of the semirigid biopolymer in the formation of highly ordered structures in living tissue such as muscle or tendon.

Acknowledgment. This work is supported by a Grant-in-Aid for the Specially Promoted Research (No. 18002002) from the Ministry of Education, Science, Sports, and Culture of Japan.

References and Notes

(1) Laufer, N. *Nature (London)* **1958**, *181*, 1338.
(2) Rees, D. A. *Adv. Carbohydr. Chem.* **1969**, *24*, 267.
(3) Duvert, M.; Bouligand, Y.; Salat, C. *Tissue Cell* **1984**, *16*, 469.
(4) Coppin, C. M.; Leavis, P. C. *Biophys. J.* **1992**, *63*, 794.
(5) Evdokimov, Y. M.; Nasedkina, T. V.; Salyanov, V. I.; Badaev, N. S. *Mol. Biol.* **1996**, *30*, 219.
(6) Petrache, H. I.; Gouliaev, N.; Tristram-Nagle, S.; Zhang, R.; Suter, R. M.; Nagle, J. F. *Phys. Rev. E* **1998**, *57*, 6.
(7) Barrat, J. L.; Boyer, D. *J. Phys. 2* **1993**, *3*, 343.
(8) Barrat, J. L.; Joanny, J. F. *Adv. Chem. Phys.* **1996**, *94*, 1.
(9) Foo, C.; Okamoto, T. K.; McBreen, J.; Lee, H. S. *J. Polym. Sci., Polym. Chem.* **1994**, *32*, 3009.
(10) Fytas, G.; Vlassopoulos, D.; Meier, G.; Likhtman, A.; Semenov. A. N. *Phys. Rev. Lett.* **1996**, *76*, 3586.
(11) Liu, T.; Rulkens, R.; Wegner, G.; Chu, B. *Macromolecules* **1998**, *31*, 6119.
(12) Rulkens, R.; Wegner, G.; Thurn-Albrecht, T. *Langmuir* **1999**, *15*, 4022.
(13) Bockstaller, M.; Kohler, W.; Wegner, G.; Fytas, G. *Macromolecules* **2001**, *34*, 6353.
(14) Aggeli, A.; Fytas, G.; Vlassopoulos, D.; McLeish, T. C. B.; Mawer, P. J.; Boden, N. *Biomacromolecules* **2001**, *2*, 378.
(15) Bockstaller, M.; Kohler, W.; Wegner, G.; Fytas, G. *Macromolecules* **2001**, *34*, 6359.
(16) Fütterer, T.; Hellweg, T.; Findenegg, G. H. *Macromolecules* **2005**, *38*, 7443.
(17) Kroeger, A.; Belack, J.; Larsen, A.; Fytas, G.; Wegner, G. *Macromolecules* **2006**, *39*, 7098.
(18) Hess, B.; Sayar, M.; Holm, C. *Macromolecules* **2007**, *40*, 1703.
(19) Kroeger, A.; Deimede, V.; Belack, J.; Lieberwirth, I.; Fytas, G.; Wegner, G. *Macromolecules* **2007**, *40*, 105.
(20) Vandenberg, E. J.; Diveley, W. R.; Filar, L. J.; Pater, S. R.; Barth, H. G. *J. Polym. Sci., Part A: Polym. Chem.* **1989**, *27*, 3745.
(21) Sarkar, N.; Kershner, L. D. *J. Appl. Polym. Sci.* **1996**, *62*, 393.
(22) Funaki, T.; Kaneko, T.; Yamaoka, K.; Ohsedo, Y.; Gong, J. P.; Osada, Y.; Shibasaki, Y.; Ueda, M. *Langmuir* **2004**, *20*, 6518.
(23) Pawlowski, W. P.; Gilbert, R. D.; Fornes, R. E.; Purrington, S. T. *J. Polym. Sci., Part B: Polym Phys.* **1988**, *26*, 1101.
(24) Blades, H. U.S. Patent 3,869,430, 1975.
(25) Shigekura, Y.; Chen, Y. M.; Furukawa, H.; Kaneko, T.; Kaneko, D.; Osada, Y.; Gong, J. P. *Adv. Mater.* **2005**, *17*, 2695.
(26) Shigekura, Y.; Furukawa, H.; Yang, W.; Chen, Y. M.; Kaneko, T.; Kaneko, D.; Osada, Y.; Gong, J. P. *Macromolecules* **2007**, *40*, 2477−2485.
(27) Furukawa, H.; Horie, K.; Nozaki, R.; Okada, M. *Phys. Rev. E* **2003**, *68*, 031406.
(28) Furukawa, H.; Hirotsu, S. *J. Phys. Soc. Jpn.* **2002**, *71*, 2873.
(29) Maestro, A.; Acharya, D. P.; Furukawa, H.; Gutiérrez, J. M.; López-Quintela, M. A.; Ishitobi, M.; Kunieda, H. *J. Phys. Chem. B* **2004**, *108*, 14009.
(30) Naga, N.; Oda, E.; Toyota, A.; Horie, K.; Furukawa, H. *Macromol. Chem. Phys.* **2006**, *207*, 627.
(31) Born, M.; Wolf, E. *Principles of Optics*; Cambridge University Press: London, 1959.
(32) Oosawa, F. *J. Polym. Sci.* **1957**, *23*, 421.
(33) Manning, G. S. *J. Chem. Phys.* **1969**, *51*, 934.

MA071251W